

# Ordered Functionalized Silica Materials with High Proton Conductivity

Roland Marschall,<sup>†</sup> Jiří Rathouský,<sup>‡</sup> and Michael Wark<sup>\*†</sup>

*Institute of Physical Chemistry and Electrochemistry, Gottfried Wilhelm Leibniz Universität Hannover, Callinstrasse 3a, 30167 Hannover, Germany, and J. Heyrovský Institute of Physical Chemistry of AS CR, v.v.i., Dolejškova 3, 18223 Prague 8, Czech Republic*

*Received April 30, 2007. Revised Manuscript Received July 27, 2007*

A simple and fast method for the preparation of the Si-MCM-41 functionalized with sulfonic acid groups (SO<sub>3</sub>H) was developed. It is based on a co-condensation synthesis and microwave treatment, which ensures an effective removal of the template (cetyltrimethylammonium bromide) and the simultaneous oxidation of thiols to SO<sub>3</sub>H groups. The obtained hybrid materials exhibit a very high proton conductivity of up to 0.2 S/cm at 100% relative humidity, which increases continuously with the temperature. The coverage of the MCM-41 pore walls with the propyl chains bearing the SO<sub>3</sub>H groups is so high that more than one SO<sub>3</sub>H group is present per nm<sup>2</sup> of the inner surface.

## 1. Introduction

The mesoporous Si-MCM-41 with its hexagonally arranged channels about 3 nm in diameter is an excellent starting material for creating hybrid organic–inorganic composites by functionalization with organic moieties with an important application potential in catalysis, separation, and nanotechnology.<sup>1</sup> We have recently shown that highly ordered mesoporous silicas functionalized with grafted sulfonic acid groups (SO<sub>3</sub>H) show promising proton conductivities for an application in fuel cell membranes operating at temperatures around 140 °C.<sup>2</sup> Such high-temperature proton exchange membrane fuel cells are highly favorable as the cooling of the fuel cell system is simplified and the tolerance toward CO is increased, which leads to a more efficient fuel cell arrangement. Recently, some first attempts to use modified Si-MCM-41 particles as inorganic additives in proton conducting membranes like Nafion or sulfonated poly(ether ketone)s (SPEEK) have been published.<sup>3,4</sup> The mesoporous additives are used to enhance the water adsorption capacity of the membranes, as a high water storage increases the proton conductivity and facilitates the water management in the final fuel cell. Thereby, the hexagonal arrangement of 1-D pores of the Si-MCM-41 and Si-SBA-15 mesoporous molecular sieves has turned out to be crucial in order to achieve a good proton conductivity. The functionalized Si-MCM-41 has proven a high capability for water

storage even at temperatures above 100 °C, especially in composite membrane applications.<sup>5</sup>

In order to enhance the degree of functionalization, the preparation employing a co-condensation of sodium metasilicate with mercaptopropyltrimethoxysilane (MPMS) as a sulfur-containing silica source is advantageous. In this contribution, we are showing that such co-condensed material containing thiol (SH) groups can be converted to the sulfonic acid group functionalized Si-MCM-41 by a new direct, simple, and fast route employing microwave irradiation for the simultaneous template removal and thiol group oxidation. The detour using a thiol silane and subsequent oxidation is necessary because a SO<sub>3</sub>H group functionalized alkoxy silane would react with each other, forming sulfonic acid esters.

The use of microwave irradiation is of advantage because the oxidation of thiol groups can be performed in one step together with the removal of the template within a very short time. Tian et al. reported that the template removal from mesoporous silica precursors by the microwave irradiation leads to higher surface areas, larger pore volumes, and higher concentrations of surface OH groups suitable for further functionalization than conventional calcination.<sup>6</sup> Microwave irradiation was mainly employed for the synthesis of zeolites (e.g., sodalite, zeolites A, Y, ZSM-5), aluminophosphates (e.g., AIPO<sub>4</sub>-5), and mesoporous materials (e.g., MCM-41, SBA-15, SBA-16).<sup>7</sup>

\* To whom correspondence should be addressed: e-mail Michael.Wark@pci.uni-hannover.de.

<sup>†</sup> Gottfried Wilhelm Leibniz Universität Hannover.

<sup>‡</sup> J. Heyrovský Institute of Physical Chemistry.

- (1) (a) Stein, A. *Adv. Mater.* **2003**, *15*, 763. (b) de, A. A.; Soler-Illia, G. J.; Sanchez, C.; Lebeau, B.; Patarin, J. *Chem. Rev.* **2002**, *102*, 4093.
- (2) Marschall, R.; Bannat, I.; Wark, M.; Caro, J. *Microporous Mesoporous Mater.* **2007**, *99*, 190.
- (3) Karthikeyan, C. S.; Nunes, S. P.; Prado, L. A. S. A.; Ponce, M. L.; Silva, H.; Ruffmann, B.; Schulte, K. *J. Membr. Sci.* **2005**, *254*, 139.
- (4) Ahmad, M. I.; Zaidi, S. M. J.; Ahmad, S. *J. Power Sources* **2006**, *157*, 35.

(5) Zaidi, S. M. J.; Ahmad, M. I. *J. Membr. Sci.* **2006**, *279*, 548.

(6) Tian, B.; Liu, X.; Yu, C.; Gao, F.; Luo, Q.; Xie, S.; Tu, B.; Zhao, D. *Chem. Commun.* **2002**, 1186.

(7) (a) Chu, P.; Dwyer, F. G.; Vartuli, J. C. US Patent 4778 666, 1988. (b) Lim, H. M.; Ahn, B. G.; Jung, S.-J.; Lee, S. H. *Adv. Technol. Mater. Mater. Process. J.* **2003**, *6*, 104. (c) Katsuki, H.; Furuta, S.; Komarneni, S. *J. Porous Mater.* **2001**, *8*, 5. (d) Girmus, I.; Jancke, K.; Vetter, R.; Richter-Mendau, J.; Caro, J. *Zeolites* **1995**, *15*, 33. (e) Wu, C. G.; Bein, T. *Chem. Commun.* **1996**, 925. (f) Newalkar, B. L.; Komarneni, S.; Katsuki, H. *Chem. Commun.* **2000**, 2389. (g) Ganschow, M.; Wark, M.; Wöhrle, D.; Schulz-Ekloff, G. *Angew. Chem., Int. Ed.* **2000**, *39*, 161. (h) Hwang, Y. K.; Chang, J.-S.; Kwon, Y.-U.; Park, S.-E. *Microporous Mesoporous Mater.* **2004**, *68*, 21.

Further, the material obtained by the novel route combining the co-condensation synthesis at moderate temperature of 100 °C and microwave treatment in the presence of hydrogen peroxide and nitric acid to oxidize the originally introduced thiol groups will be shown to exhibit very high proton conductivities at differing relative humidity.

## 2. Experimental Details

Thiol-functionalized Si-MCM-41 was synthesized following the homogeneous precipitation procedure published in ref 8; however, a certain percentage (20, 30, and 40 mol %) of the silica source sodium metasilicate (NaSiO<sub>3</sub>, Aldrich) was replaced by 3-mercaptopropyltrimethoxysilane (MPMS, Merck). In a typical synthesis, 2.61 g of cetyltrimethylammonium bromide (CTAB, Aldrich) was dissolved in 400 mL of deionized water at 30 °C. After the complete dissolution of the surfactant, sodium metasilicate followed with MPMS was added under stirring. The molar ratio of the individual components of the reaction mixture was 1 (CTAB):3103 (H<sub>2</sub>O):3.05 -  $x$  (Na silicate): $x$  (MPMS) with  $x$  either 0, 0.61, 0.92, or 1.22. Finally, 4 mL of ethyl acetate was added under vigorous stirring, whose hydrolysis to acetic acid ensures highly homogeneous acidification of the reaction mixture and consequently a uniform hydrolysis–condensation reaction of metasilicate and MPMS. After 15 s, the stirring was stopped and the solution was kept still for 24 h at room temperature in a closed PE bottle. The final pH was around 9.9 for a typical synthesis. Hydrothermal treatment was carried out for an additional 24 h at 100 °C. The white precipitate was recovered by filtration and washed with ethanol and water. Samples were dried at room temperature overnight. Microwave treatment for template removal and simultaneous thiol oxidation was carried out using an Ethos 1 microwave system (MLS) in Teflon reaction vessels, which are transparent for the microwave radiation. 0.1 g of the as-synthesized powder was suspended in a mixture of HNO<sub>3</sub> (65%, Roth) and H<sub>2</sub>O<sub>2</sub> (30%, Roth). The mixture was treated by continuous microwave irradiation (maximum 600 W) for up to 5 min at 200 °C, the maximum internal pressure being 18 bar.

The samples prepared using 20, 30, and 40 mol % of MPMS are designated as 20, 30, and 40% SO<sub>3</sub>H-MCM-41, respectively. The attached indication in the parentheses (mw), (extr), and (calc) corresponds to the samples which were treated by the microwave irradiation, extracted with boiling ethanol (refluxing for 24 h), or calcined at 600 °C for 20 h (heating/cooling rate of 1 K/min), respectively.

Macroporous silica gel Davisil (Supelco) was functionalized with MPMS by the grafting method previously reported.<sup>2</sup> To 0.5 g of the silica gel powder suspended in 20 mL of dichloromethane 0.94 mL (10 mmol/g) or 1.88 mL (20 mmol/g) of MPMS were added at 0 °C under an argon atmosphere. The mixture was stirred for 22 h while the cooling bath was not renewed. After filtration the samples were washed with dichloromethane and ethanol. Thiol group oxidation was performed in hydrogen peroxide during 48 h subsequent stirring in sulfuric acid (1 M) for several hours.

Nitrogen adsorption experiments at the boiling point of nitrogen (ca. -196 °C) were carried out with a Micromeritics ASAP 2010 apparatus. Prior to each adsorption measurement, samples were outgassed at 150 °C overnight. X-ray diffraction (XRD) was measured with a Philips X'pert diffractometer at room temperature in the range from 1° to 10° 2 $\theta$ , using Cu K $\alpha$  radiation. Fourier-transform infrared (FT-IR) spectra of functionalized powders were

recorded in the attenuated total reflection mode on a diamond crystal using a Bruker Tensor 27 instrument (resolution: 2 cm<sup>-1</sup>, 200 scans) in the range of 400–4000 cm<sup>-1</sup>. Thermogravimetric measurements (differential thermal analysis, DTA) were carried out between 20 and 1000 °C using a Netzsch Simultaneous Thermal Analyzer 429 with a heating rate of 5 °C/min in air.

The proton conductivity was measured by impedance spectroscopy (IS) using a Zahner electrochemical workstation IM6e in a frequency range from 1 to 10<sup>6</sup> Hz with an oscillating voltage of 100 mV. Prior to the measurement, the functionalized powders were pressed into small pellets 8 mm in diameter and 0.5–1 mm in thickness, which were inserted between two thin graphite slices (8 mm in diameter). Afterward, they were put into a PTFE specimen holder, which was located in a gastight stainless steel body with thermocouple access to the holder. This body was connected via a stainless steel tube to a stainless steel water reservoir. Relative humidity (RH) in the cell was controlled by adjusting the temperature of the water tank. The specific conductivity was calculated according to the formula  $\sigma = (1/R)(L/A)$ , where  $R$  is the resistance corresponding to the phase angle closest to zero in the Bode diagram,  $L$  the thickness of the sample between the electrodes, and  $A$  the cross-sectional contact area of the electrodes. This analysis procedure is typically used to interpret proton conductivities in powders or membranes.<sup>9</sup>

The ion exchange capacity was determined by titration. A small amount of functionalized powder was suspended in a 0.01 M sodium hydroxide solution for 48 h, the remaining sodium hydroxide being titrated with hydrochloric acid.

## 3. Results and Discussion

In order to obtain a deeper insight into the process of the removal of the template and the oxidation of thiol groups, the prepared hybrid materials were investigated by FT-IR spectroscopy and thermogravimetry.

FT-IR spectroscopy evidence the template removal in the microwave oven simultaneously with the oxidation of the thiol groups to SO<sub>3</sub>H ones. After microwave treatment two peaks corresponding to sulfonate stretching vibrations appear in the region from 1100 to 1300 cm<sup>-1</sup> ( $\nu_{\max}/\text{cm}^{-1}$  1145 and 1201 (-SO<sub>2</sub>-OR)<sup>10</sup>) (Figure 1) instead of the S-H vibration at 2580 cm<sup>-1</sup>, which has almost completely disappeared. The IR signal in the 2850–3000 cm<sup>-1</sup> region resulting from C-H stretching vibrations of aliphatic CH<sub>2</sub> groups narrows and loses much intensity, indicating the contribution of the template to the signal has vanished and only the propyl groups in the anchored MPMS moieties contribute to the signal.

Thermogravimetric measurements of the oxidized samples also confirm these results. The extent of thiol group oxidation was estimated from the change in the decomposition temperatures. Thiol group decomposition starts at about 330 °C, whereas side chains with SO<sub>3</sub>H groups start to decompose at temperature as high as about 375 °C, as determined for samples containing exclusively thiol or SO<sub>3</sub>H groups (Figure 2). If both groups are present in a sample due to incomplete oxidation, the decomposition temperatures were found shifted toward higher values.<sup>2</sup> While for 20% SO<sub>3</sub>H-MCM-41 (mw)

(9) Mikhailenko, S.; Desplandier-Giscard, D.; Danumah, C.; Kaliaguine, S. *Microporous Mesoporous Mater.* **2005**, *54*, 29.

(10) Hesse, M.; Meier, H.; Zeeh, B. *Spektroskopische Methoden in der Organischen Chemie*, 6th ed.; Thieme: Stuttgart, 2002.

(8) Rathousky, J.; Zukalova, M.; Zukal, A.; Had, J. *Collect. Czech. Chem. Commun.* **1998**, *63*, 1893.

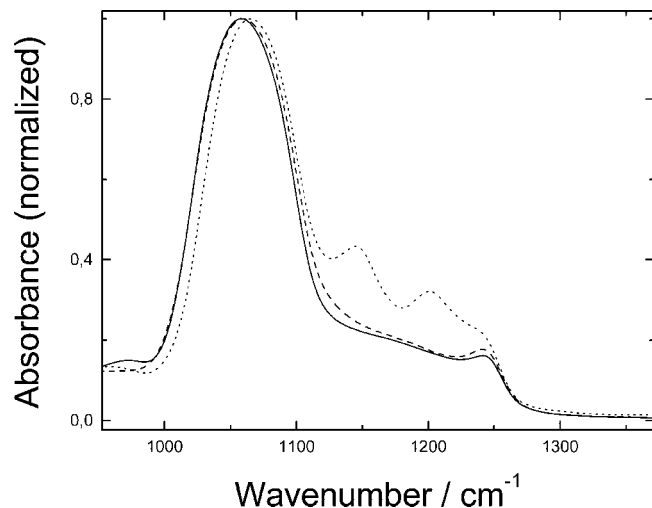


**Figure 1.** FT-IR spectra of pure Si-MCM-41 (straight line), functionalized with thiol groups, 20% SH-MCM-41 (dashed line), and after microwave oxidation (dotted line), 20% SO<sub>3</sub>H-MCM-41 (mw).

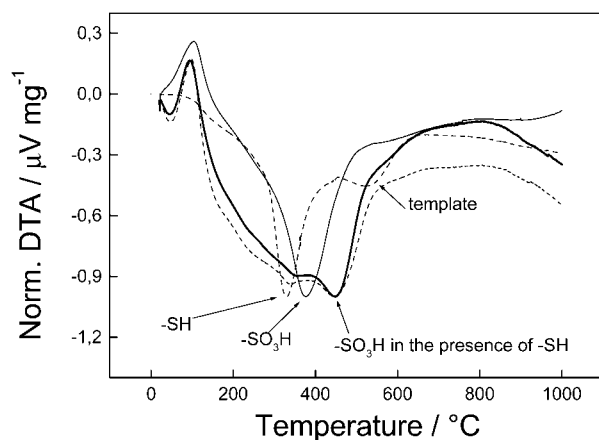


**Figure 2.** DTA curves, normalized by the largest signal. 20% SH-MCM-41 (extr) (dashed); 20% SO<sub>3</sub>H-MCM-41 (mw) (black); 30% SO<sub>3</sub>H-MCM-41 (mw) (dashed, gray); 40% SO<sub>3</sub>H-MCM-41 (mw) (gray).

full oxidation is achieved by the given procedure, the 30% and 40% SO<sub>3</sub>H-MCM-41 (mw) still contain small amounts of thiol groups (Figure 2). Compared to the extracted 20% SH-MCM-41 (extr), the microwave treated 20% SO<sub>3</sub>H-MCM-41 (mw) shows no more template signal, indicating a complete template removal by microwave irradiation unlike the ethanol extraction.

The texture properties of the prepared samples were determined by the analysis of the adsorption isotherms of N<sub>2</sub> at the boiling point of liquid nitrogen (Figure 3). Pristine Si-MCM-41 material synthesized by the homogeneous precipitation without adding MPMS exhibits the typical steep increase in the adsorption at the relative pressure  $P/P_0$  of 0.27–0.34, which is due to the reversible capillary condensation within the Si-MCM-41 mesopores ca. 3 nm in diameter. The broad hysteresis at  $P/P_0$  from 0.5 to 1 is due to the presence of some imperfections and cracks within the particles of this material. The BET surface area, pore volume, pore size, and the BET  $C$  constant of the Si-MCM-41 achieve 1030 m<sup>2</sup> g<sup>-1</sup>, 0.954 cm<sup>3</sup> g<sup>-1</sup>, 2.7 nm, and 78, respectively. Whether the template has been removed by the calcination

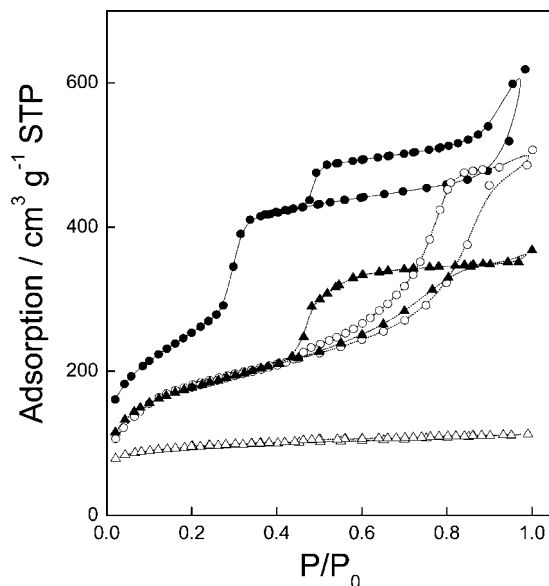


**Figure 3.** Nitrogen sorption isotherms on the pristine Si-MCM-41 (•) and on functionalized samples 20 (○), 30 (▲), and 40% (△) SO<sub>3</sub>H-MCM-41 (mw).

or microwave treatment has no effect on the texture properties of the pristine material.<sup>4</sup>

The addition of MPMS to the reaction mixture for the preparation of the functionalized Si-MCM-41 has had a profound effect on the texture properties (Figure 3). The isotherms for the 20% and 30% SO<sub>3</sub>H-MCM-41 (mw) exhibit variously shaped hysteresis loops corresponding to differently sized mesopores. On the contrary, the isotherm for the 40% SO<sub>3</sub>H-MCM-41 shows more or less horizontal plateau after a steep increase in adsorption at very low relative pressures. The BET surface areas and the BET  $C$  constants for 20% and 30% SO<sub>3</sub>H-MCM-41 (mw) samples equal 645 and 625 m<sup>2</sup> g<sup>-1</sup> and 140 and 347, respectively. For the 40% SO<sub>3</sub>H-MCM-41 sample the BET equation does not hold, which indicates the microporous nature of this sample.

Because of the complex nature of functionalized materials, the comparative plot method has been chosen for the analysis of their texture properties using two fundamentally different reference materials. In these plots, the adsorption on the material under study is plotted against that on a well-defined and characterized reference material at the same relative pressure. As the first reference material, the pristine Si-MCM-41 molecular sieve has been used, whose pore architecture should be comparable to those of the functionalized materials. A functionalized macroporous silica gel Davisil (Supelco) with the BET surface area of 82.8 m<sup>2</sup>/g served as the second reference. The pristine silica gel was functionalized with 10 and 20 mmol of MPMS and 10 and 20 mmol of SO<sub>3</sub>H-PMS. The adsorption isotherms on all these materials relating to 1 m<sup>2</sup> of their BET surface area are shown in Figure 4. The functionalization does not have practically any effect on the surface area, but the strength of the interaction of nitrogen molecules with the surface substantially depends on its chemical nature. The BET  $C$  constant for thiol-functionalized materials is much lower than that for the pristine Davisil (64–76 vs 112), while for SO<sub>3</sub>H-functionalized ones sub-

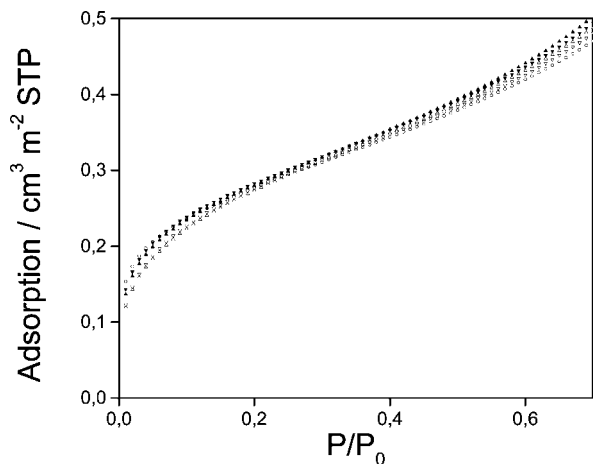


**Figure 4.** Adsorption isotherms of nitrogen on macroporous silica gel Davisil (O) and its functionalized forms: 10 mmol -SH ( $\Delta$ ), 20 mmol -SH ( $\nabla$ ), 10 mmol -SO<sub>3</sub>H ( $\blacktriangle$ ), and 20 mmol -SO<sub>3</sub>H ( $\blacktriangledown$ ). The adsorption is related to 1 m<sup>2</sup> of the BET surface area.

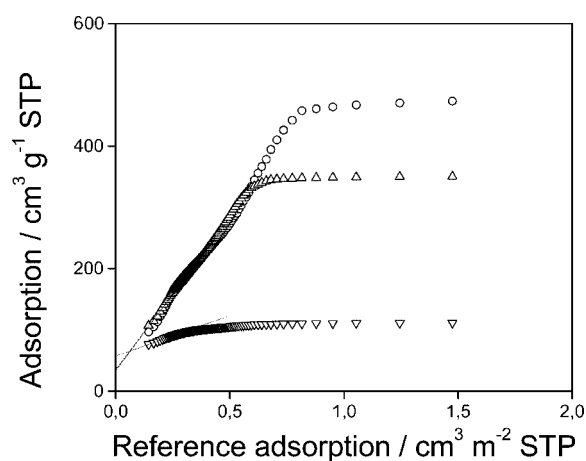


**Figure 5.** Comparative plots for 20% (O), 30% ( $\Delta$ ) and 40% ( $\nabla$ ) SO<sub>3</sub>H-MCM-41 (mw). The isotherm obtained on the 20 mmol -SO<sub>3</sub>H Davisil silica gel serves as the reference adsorption.

stantial increase has been observed, achieving for the 20 mmol SO<sub>3</sub>H-sample even 138. This indicates strong interaction of nitrogen molecules with the surface densely covered with SO<sub>3</sub>H groups. Because of the generally high values of the *C* constant for functionalized samples, the 20 mmol SO<sub>3</sub>H reference material has been used for the construction of the comparative plots (Figure 5). If the plots for all the three samples were extrapolated to the zero reference adsorption, there are positive intercepts on the y-axis. This confirms that all the samples contain some proportion of micropores, that for the 40% SO<sub>3</sub>H-MCM-41 (mw) being the largest. Additionally, the long linear increase of the plots for 20% and 30% SO<sub>3</sub>H-MCM-41 (mw) evidences the chemical similarity of the surface with that of the reference Davisil silica gel functionalized with SO<sub>3</sub>H groups and the presence of pores larger than micropores, such as small mesopores (see below). For the 40% SO<sub>3</sub>H-MCM-41 (mw) sample the linear increase is very short and flattens off very early, which is due to the practically exclusive presence of micropores. An important conclusion can be drawn from the comparison of the BET *C* constants for the 20 mmol SO<sub>3</sub>H-Davisil silica gel and 20% and 30% SO<sub>3</sub>H-MCM-41 (mw). While these constants are practically the same for the modified Davisil sample and

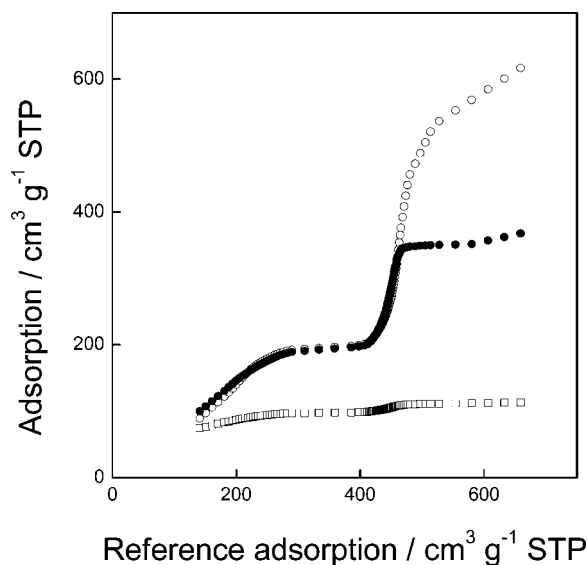


**Figure 6.** Comparative plots for functionalized samples 20 (O), 30 (●), and 40% (□) SO<sub>3</sub>H-MCM-41 (mw). The isotherm obtained on the pristine Si-MCM-41 serves as the reference adsorption.

the 20% SO<sub>3</sub>H-MCM-41 (mw), i.e., enhanced in comparison with pristine samples, the value for the 30% SO<sub>3</sub>H-MCM-41 (mw) is markedly higher (347 vs 138–140). This drastic enhancement is clearly due to the higher density of the SO<sub>3</sub>H groups on the surface of 30% SO<sub>3</sub>H-MCM-41 (mw).

To analyze the texture properties of functionalized MCM-41 samples in detail, the comparative plots were constructed, in which the adsorption on the modified Si-MCM-41 samples was compared with that on the pristine Si-MCM-41 at the same relative pressures (Figure 6). Three regions can be clearly distinguished in these plots, at the adsorption on the reference Si-MCM-41 of up to 290, from 290 to 410, and over 410 cm<sup>3</sup> g<sup>-1</sup> STP, respectively, which corresponds to the relative pressure <0.27, 0.27–0.34, and >0.34. In the first region, the plots for all the three samples are increasing roughly linearly, but the plausibility is doubtful due to the different chemical nature of both the modified and reference MCM-41 materials. In the second region at the adsorption on the reference Si-MCM-41 of 290–410 cm<sup>3</sup> g<sup>-1</sup> STP, the plots for all the samples are almost perfectly horizontal. Consequently, the adsorption in this region of the relative pressure, which corresponds to the steep increase for the pristine Si-MCM-41, is practically negligible. The clear reason is the narrowing of the mesopores corresponding to the Si-MCM-41 structure and their transformation to micropores or small mesopores ca. 2 nm in diameter. This phenomenon is especially prominent for the 40% SO<sub>3</sub>H-MCM-41 (mw). The pore size calculated from the pore volume and the Langmuir surface area (the BET equation does not hold for such small pores) is about 1.5 nm. Assuming a chain length of 0.6 nm for the (CH<sub>2</sub>)<sub>3</sub>-SO<sub>3</sub> chain, then by subtracting twice the chain length from the diameter of the pores of the pristine MCM-41 (2.7 nm) the size of the micropores should be roughly 1.5 nm, which is really the case. This conclusion is also in agreement with Lim et al., who established a high pore filling of the Si-MCM-41 with MPMS which results in a pore diameter of about

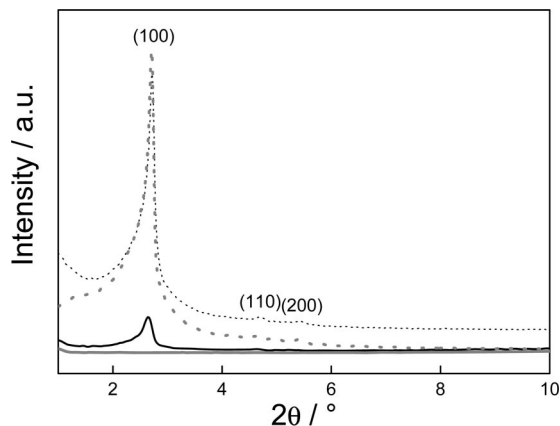


**Figure 7.** X-ray diffractograms for 20% (black) and (gray) 40% SO<sub>3</sub>H-MCM-41 (mw) samples and for calcined 20% (black, short dots) and 40% (gray, short dots) SO<sub>3</sub>H-MCM-41 (calc) samples.

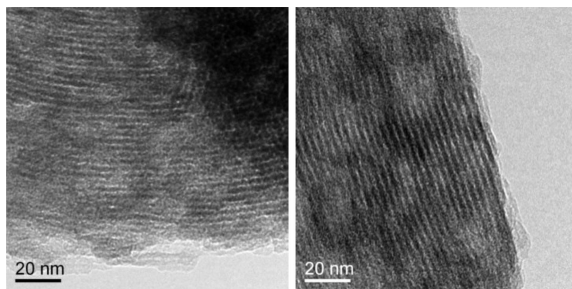


**Figure 8.** TEM images for 40% SO<sub>3</sub>H-MCM-41 (mw).

1.4 nm.<sup>11</sup> Finally, at even higher relative pressures a substantial increase in the adsorption on 20% and 30% SO<sub>3</sub>H-MCM-41 (mw) samples was observed, which is due to some parasitic mesopores or defects formed within these materials. The 40% SO<sub>3</sub>H-MCM-41 (mw) sample contains a much smaller percentage of these pores.

Figure 7 shows the X-ray powder diffractograms (XRD) for functionalized 20% and 40% SO<sub>3</sub>H-MCM-41 (mw) samples. The diffractogram for 20% SO<sub>3</sub>H-MCM-41 (mw) exhibits a drastically diminished (100) reflection and an almost complete absence of the (110) and (200) reflections. Finally, no reflections have been observed at all. This confirms the substantial (for 20% SO<sub>3</sub>H-MCM-41 (mw)) or practically complete (for 40% SO<sub>3</sub>H-MCM-41 (mw)) filling of the Si-MCM-41 pores in the functionalized and microwave-treated mesoporous materials. As the presence of organic groups in the pores lowers the electron density contrast between the pores and walls, the reflection intensity is decreased.<sup>12</sup> The X-ray diffraction patterns measured after the complete removal of the organic matter by calcinations show the expected three well-resolved reflexes for the Si-MCM-41 (Figure 7).

The high regularity of the pore ordering for the functionalized SO<sub>3</sub>H-MCM-41 (mw) samples was also confirmed by transmission electron microscopy (TEM). The TEM micrographs in Figure 8 clearly show the pore arrangement characteristic for the Si-MCM-41 structure obtained for the 40% SO<sub>3</sub>H-MCM-41 (mw) sample.

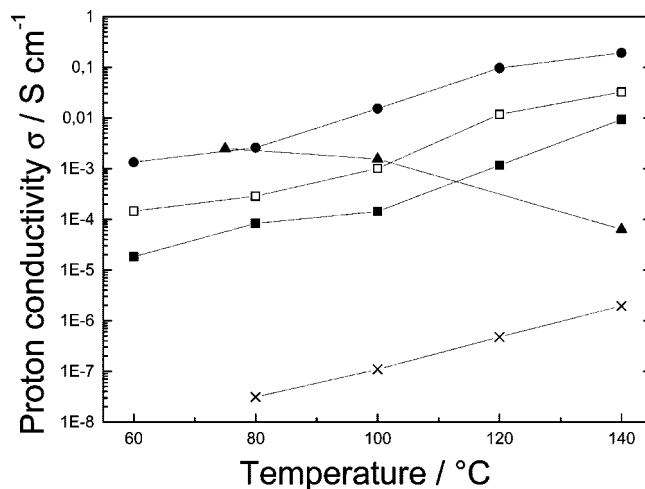


**Figure 9.** Proton conductivity  $\sigma$  measured at 100% RH for 0% (x), 20% (■), 30% (□), and 40% (●) SO<sub>3</sub>H-MCM-41 (mw) and for Nafion (▲).

Figure 9 shows that the proton conductivity of all samples increases continuously with temperature. Proton conductivity in the presence of water is due to the so-called Grotthuss mechanism.<sup>13</sup> In this mechanism, the proton transport is mainly caused by the hopping of the protons from one water molecule to another. To a smaller extent, also the diffusion of H<sub>3</sub>O<sup>+</sup> ions enhances the proton transport.

The increase in temperature strongly affects both mechanisms; hopping as well as diffusion becomes faster. Furthermore, because the anchoring propyl chains rotate and vibrate more easily, the SO<sub>3</sub>H groups at the end of the chains can easier encounter each other, and thus the direct proton transport is facilitated.

It is remarkable that in contrast to Nafion foils, for which the proton conductivity decreases drastically above 100 °C due to the water loss,<sup>14,15</sup> water seems to be kept inside the channels. The channel geometry of the pores, in which the sulfonic acid groups are fixed, does not only help to keep water but also supports the guidance of the protons through the tested pellets.

The proton conductivity also increases with the extent of substitution of metasilicate by MPMS in the co-condensation synthesis. The highest proton conductivity of 0.2 S/cm is achieved with the 40% SO<sub>3</sub>H-MCM-41 (mw) sample due to the very high pore filling with SO<sub>3</sub>H groups and the absence of any parasitic pores, which adversely affect the pellet conductivity.

Pristine Si-MCM-41 alone shows only a negligible proton conductivity of about 10<sup>-6</sup> S/cm, which results from a partial dissociation of water molecules in the presence of silanol groups, which are present overall on the surface, leading to an increased charge carrier concentration close to the inner surface.<sup>9</sup>

Figure 10 confirms the influence of water and the propyl -SO<sub>3</sub>H chains in the proton conductivity of the synthesized

(11) Lim, M. H.; Blanford, C. F.; Stein, A. *Chem. Mater.* **1998**, *10*, 467.

(12) Marler, B.; Oberhagemann, U.; Vortmann, S.; Gies, H. *Microporous Mater.* **1996**, *6*, 375.

(13) van Grotthus, C. J. D. *Ann. Chim.* **1806**, *58*, 54.

(14) Hogarth, M.; Glipe, X. ETSU Technical Report F/02/00189/REP, **2001**.

(15) Marschall, R.; Wark, M.; Jeske, M.; Wilhelm, M.; Grathwohl, G.; Caro, J. *Stud. Surf. Sci. Catal., Proc. 15th Int. Zeolite Conf.* **2007**, in press.

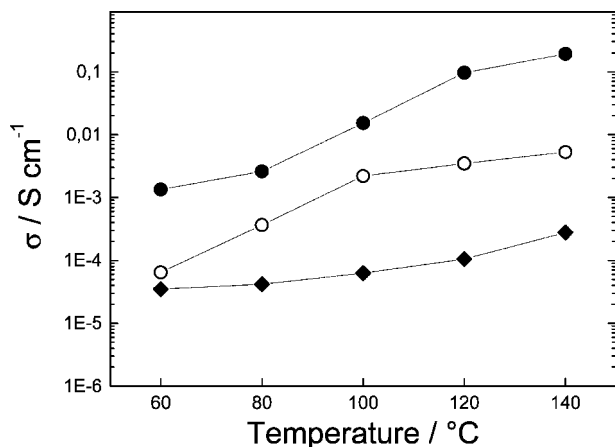


**Figure 10.** Proton conductivity  $\sigma$  of 40%  $\text{SO}_3\text{H}$ -MCM-41 (mw) at 0% ( $\blacklozenge$ ), 50% ( $\circ$ ), and 100% ( $\bullet$ ) RH.

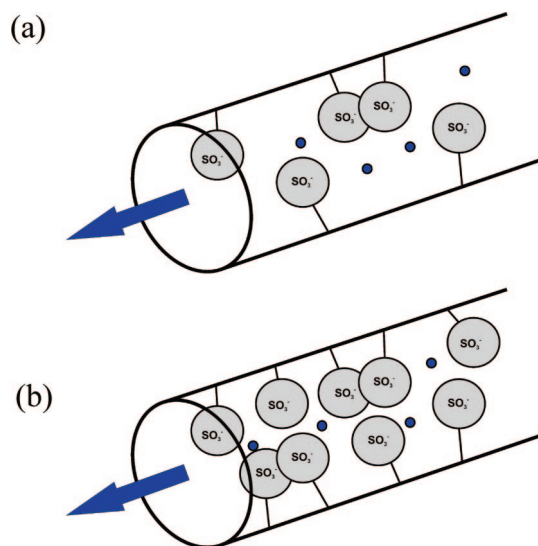
samples. The 40%  $\text{SO}_3\text{H}$ -MCM-41 (mw) sample has been measured under different RH to show increasing proton conductivity performance by increasing the RH in the measurement cell.

The proton conductivity of the 40%  $\text{SO}_3\text{H}$ -MCM-41 (mw) materials drastically increases with the increasing relative humidity. However, the data in Figure 10 show a good intrinsic proton conductivity even without any additional water in the gas atmosphere ( $10^{-5}$ – $10^{-4}$  S/cm). This result also confirms the proposed Grotthus-like mechanism, where the proton hopping from one water molecule to another is additionally supported by the propyl  $-\text{SO}_3\text{H}$  groups.

Compared to materials functionalized by grafting with MPMS,<sup>2</sup> the loading of samples prepared in this study by co-condensation is much higher, and therefore the proton conductivity is increased by 2 orders of magnitude. The ion exchange capacity (IEC) gives the concentration of  $\text{SO}_3\text{H}$  groups in the samples. While it does not exceed 1 mmol/g for the  $\text{SO}_3\text{H}$ -MCM-41 hybrid materials prepared by grafting, for those synthesized by co-condensation it achieves up to 2.3 mmol/g of  $\text{SO}_3\text{H}$  groups accessible for ion exchange in 40%  $\text{SO}_3\text{H}$ -MCM-41 (mw). This value is much higher than that found by Lim et al.<sup>11</sup> of 1.76 mmol/g, although these authors report a sulfur content of 4.7 mmol/g. In contrast to our material, in their work most of the sulfur seems to be buried in the walls.

If one assumes that in the grafting process (i) the Si-MCM-41 exhibits a surface area of 1000  $\text{m}^2/\text{g}$ , (ii) the average density of OH groups on its surface is about 3 per square nanometer,<sup>16,17</sup> and (iii) every MPMS is attached by reacting with three OH groups, roughly a maximal loading of  $\text{SO}_3\text{H}$  groups of 1.67 mmol/g results. The fact that the loading, which has been really achieved by grafting, is lower indicates that blocking effects and hindrance of MPMS diffusion in the pores impede the grafting process. Because in the co-condensation process these limitations are removed, loadings of up to 1.4  $\text{SO}_3\text{H}$  groups per  $\text{nm}^2$  can be realized document-

**Scheme 1. Schematic Comparison of the Loading of  $\text{SO}_3\text{H}$  Groups within the Pores of the Si-MCM-41 by (a) Grafting and (b) Co-condensation<sup>a</sup>**



<sup>a</sup> The lines connecting the walls and the  $\text{SO}_3\text{H}$  groups schematically denote the flexible propyl chains.

ing that the MPMS on average binds with fewer than three groups. It is noteworthy that the IEC does not follow linearly the amount of MPMS offered in the co-condensation synthesis. This indicates that at a higher offer of MPMS increasing amounts of thiol groups are buried inaccessibly within the pore walls and explains why in the 30% and 40% samples also thiol groups were detected by DTA measurements (Figure 2).

Scheme 1 illustrates the situation inside the pores of functionalized MCM-41; the higher pore filling in samples synthesized by co-condensation being helpful for a better guidance of protons through the narrowed pore channels. Furthermore, less water is sufficient to achieve a similar extent of proton transport because the sulfonic acid groups are closer together. This renders these hybrid samples good candidates for an application as additives in fuel cell membranes operating at temperatures of around 140 °C.

#### 4. Conclusions

In summary, a simple and fast method for the preparation of  $\text{SO}_3\text{H}$ -functionalized Si-MCM-41 samples by co-condensation synthesis and microwave treatment for an effective template removal with the simultaneous thiol to  $\text{SO}_3\text{H}$  group oxidation has been presented. Pellets pressed from the synthesized powders showed very high proton conductivities of up to 0.2 S/cm at 100% RH. Whereas for other kinds of proton conducting membranes, e.g., Nafion, the proton conductivity decreases drastically with temperature, the proton conductivity of these materials increases continuously with temperature. The high loading with organic moieties achieved by the co-condensation synthesis turned out to be a crucial advantage of this method compared to the postsynthetic grafting. The pore filling is increased in such a large extent that more than one  $\text{SO}_3\text{H}$  group is present per  $\text{nm}^2$  of

(16) Ishikawa, T.; Matsuda, M.; Yasukawa, A.; Kandori, K.; Inagaki, S.; Fukushima, T.; Kondo, S. *J. Chem. Soc., Faraday Trans.* **1996**, *92*, 1985.

(17) Zhao, X.; Lu, G.; Whittaker, A.; Millar, G.; Zhu, H. *J. Phys. Chem. B* **1997**, *101*, 6525.

inner surface. The high IEC as well as the absence of larger unfilled parasitic pores enhance the guided proton transport through the pore channels, resulting in proton conductivities in the range of those of the most promising solid proton conductors like heteropolyacids or solid boron phosphates.<sup>18–21</sup>

**Acknowledgment.** The work was supported by the Deutsche Forschungsgemeinschaft (DFG) (CA 147/13-1, SPP1181). The authors thank Inga Bannat (Institute of Physical Chemistry, Leibniz University Hannover) for TEM measurements and Falk Heinroth (Institute of Inorganic Chemistry, Leibniz University

Hannover) for TGA/DTA measurements. Roland Marschall gratefully acknowledges a Georg-Christoph-Lichtenberg scholarship by the Ministry of Science and Culture of the German State of Lower Saxony.

CM071164I

- 
- (18) Kim, Y. S.; Wang, F.; Hickner, M.; Zawodzinski, T. A.; McGrath, J. E. *J. Membr. Sci.* **2003**, *212*, 263.  
(19) Mikhailenko, S. D.; Zaidi, S. M. J.; Kaliaguine, S. *J. Chem. Soc., Faraday Trans.* **1998**, *94*, 1613.  
(20) Mikhailenko, S. D.; Zaidi, S. M. J.; Kaliaguine, S. *Catal. Today* **2001**, *67*, 225.  
(21) Zaidi, S. M. J.; Mikhailenko, S. D.; Robertson, G. P.; Guiver, M. D.; Kaliaguine, S. *J. Membr. Sci.* **2000**, *173*, 17.